polymer

Synthesis and fractionation of syndiotactic-polystyrene/polyethylene copolymers with $C_5H_5TiCl_3$ catalysts

P.P. Chu[*], H.S. Tseng, Y.P. Chen, D.D. Yu

Department of Chemistry, National Central University, Chung-Li, Taiwan, ROC 32054

Abstract

Highly stereoregulated syndiotactic-polystyrene/polyethylene (s-PS/PE) block copolymers with variable ethylene block lengths are synthesized using the sequential monomer feed scheme with $C_5H_5TiCl_3$ catalyst. The copolymer, after removing the atactic portion, is separated into two fractions by tetrahydrofuran (THF). The insoluble fraction contains a highly stereoregulated s-PS block linked with PE blocks, while the soluble fraction also contains a highly stereoregulated s-PS block but separated randomly by a shorter or isolated ethylene unit. For the I-fraction, $r_E = 25 \pm 5$ and $r_S = 1.9 \pm 0.3$, and for the S-fraction $r_E = 0.4 \pm 0.1$ and $r_S = 0.34 \pm 0.15$. These results are compared with prior studies, where mainly random type PS/PE copolymers with low styrene stereoregularity and rigio-irregular styrene and polyethylene are produced. Apparently, both the sequential feed scheme coupled with the use of a lower reactivity metallocene catalyst facilitated the switching of catalytical sites with the majority product being of block nature. © 2000 Elsevier Science Ltd. All rights reserved.

Keywords: Sequential monomer feed scheme; $C_5H_5TiCl_3$; Syndiotactic-polystyrene/polyethylene

1. Introduction

Advantages of metallocene catalysts over conventional Ziegler–Natta catalysts include stereospecific features, superb activity with true single-site formation, well-defined polymer microstructure and the versatility of catalyst structure. Recently, the copolymerization of olefins with metallocene catalysts has attracted interests that include copolymerizing with a soft polymer segment such as ethylene, butadiene and hexene [1–5]. Zambelli et al. have demonstrated that by using the Ti or Zr metallocenes activated with methylalumoxane (MAO) [6], styrene–ethylene copolymer can be produced at high temperatures. The product is mostly atactic with random ethylene insertion. Mulhaupt et al. reported that bis(phenolate) complexes of titanium produce random poly(ethene-*co*-styrene) copolymer [7]. Ren et al. showed, by using isopropyldine(cyclopentadienyl)(9-fluorrenyl)zirconium dichloride, that styrene monomer is randomly dispersed in ethylene chain and reduces ethylene crystallinity [8]. Using $C_5H_5Ti(OPh)_3$, Xu et al. reported the synthesis of elastoplastic and amorphous styrene–ethylene copolymers where the styrene block is mostly atactic with random ethylene insertion [9]. Minor side products from such copolymerization are the s-PS homopolymer having regio-irregular segments and the PE homopolymer. In all these attempts, "true" s-PS/PE copolymers with a highly syndiotactic styrene block chemically bonded with polyethylene is yet to be reported. An earlier study using the same catalyst, $C_5H_5TiCl_3$, has produced dual components of s-PS and PE blends [10]. Oliva et al. used the same catalyst to prepare random S–E copolymers with some regio-irreguar units at 20°C at an ethylene pressure range of 20–50 psi [11]. All previous copolymerization studies demonstrated that the switching between α-olefin commoner units during polymerization is possible. Taking into consideration the large differences of reactivities between ethylene and styrene, a true s-PS/PE copolymer with a long s-PS block can be synthesized with a sequential feed scheme under low ethylene pressure, high MAO content and possibly at low reaction temperatures. The main challenge, however, is to attain a long enough ethylene block attached to the styrene block before chain transfer occurs. This study presents the results of s-PS/PE block copolymers with sequential feed schemes and the fraction that resolves the product mixture. Major focuses would be to examine the reactivity and conditions under which the s-PS/PE copolymers may be produced; possible reaction mechanisms are also discussed.

* Corresponding author. Tel.: + 886-3-425-8631; fax: + 886-3-422-7664.

E-mail address: pjchu@rs970.ncu.edu.tw (P.P. Chu).

Table 1
Polymerization reaction condition and activity

Run no	Ethylene pressure	Styrene (mol/l)	Temperature (°C)	Activity $\times 10^{-5}$ (g/Ti mol $\times$ h)
1	0	2.0	30	1.007
2	5	2.0	30	0.586
3	10	2.0	30	0.840
4	15	2.0	30	0.944
5	20	2.0	30	0.745
6	30	2.0	30	0.375
7	10	3.0	30	0.855
8	10	3.5	30	0.937
9	10	4.0	30	1.070
10	10	5.0	30	2.466
11	5	2.0	15	0.743
12	5	2.0	50	1.171

2. Experimental

2.1. Materials

Polymerization-grade ethylene and extra pure grade nitrogen were purified prior to use. Styrene was purified by distillation under reduced pressure over CaH_2. Toluene was refluxed over metallic sodium/benzophenone for 24 h and distilled under a nitrogen atmosphere. $C_5H_5TiCl_3$ was either obtained commercially from Aldrich without further purification, or prepared according to the literature procedure.[12] Methylaluminoxane was obtained from Albemarle Cooperation and used directly.

2.2. Copolymerization

The present copolymerization was performed in a stainless steel reactor. Metallocene/MAO co-catalyst toluene solution (mol ratio 1:1300) was first activated in the closed vessel for over 20 min, the styrene solution was injected first into the nitrogen-purged reactor, and reacted for 15 min followed by ethylene injection. Ethylene was fed continuously under a constant pressure (controlled to within 0.2 psi) during the full course of the reaction. The reactor temperature was kept below 50°C and controlled to within ±0.5°C and reacted for 4 h. Upon completion, the reactor was degassed and the reaction terminated by addition of diluted hydrochloric acid (with methanol). The copolymer product was precipitated with further addition of methanol.

2.3. Solvent fractionation

The copolymers were first extracted in cellulose thimble filler with boiling methyl ethyl ketone (MEK) for 12 h in Soxhlet apparatus. After removing the atactic polystyrene, the product was boiled in tetrahydrofuran (THF) for an additional 24 h. THF-soluble extract (S-fraction contains random s-PS/PE copolymer) was recovered by evaporation of the solvent and the remaining insoluble portion (I-fraction) was collected. Both S- and I-fractions were desiccated

in a vacuum oven, weighted and characterized subsequently.

2.4. Characterization

Gel permeation chromatography (GPC) analysis was conducted on Waters GPC, using 1,2,4 trichlorobenzene (TCB) as the eluent at 130°C. Solution ^{13}C NMR spectra were recorded on a Bruker AM 400 spectrometer operating at 100.1 MHz at 100°C in TCB solution (b.p. = 165°C), with d-Benzene as the lock solvent. Styrene tacticity was determined from the (mm), (mr) and (rr) triad concentrations determined from NMR resonance of the α-carbon located at ~146 ppm using the relationship: [rr] = (rr)/[(mm) + (mr) + (rr)]. Percentage racemic content was calculated as [r] = [rr] + 0.5[mr] [13]. Differential scanning calorimeter measurements were conducted with a Perkin–Elmer DSC 7 series, with a 10 ml/min flow of dry nitrogen purge for both samples and the reference cells. The measurement was made with 3–4 mg samples on a DSC plate after cooling the specimens to 0°C following the first scan. The scan rate was 10°C/min within the temperature range of 0–300°C. Thermogravimetric analysis (TGA) was obtained with a Perkin–Elmer TGA 7 analyzer at a scan rate of 10°C/min, operated under dry-nitrogen purge.

3. Results

3.1. Reactivity

Copolymerization of styrene and ethylene was conducted under varying ethylene pressure, reaction temperature and styrene concentration in the presence of $C_5H_5TiCl_3$/MAO. Unlike other copolymerizations, styrene was reacted first followed by sequential feeding of ethylene. Consistent with previous styrene/ethylene copolymerization studies, a large surplus of styrene in the monomer feed ratio is required to produce a reasonable amount of styrene in the copolymers.

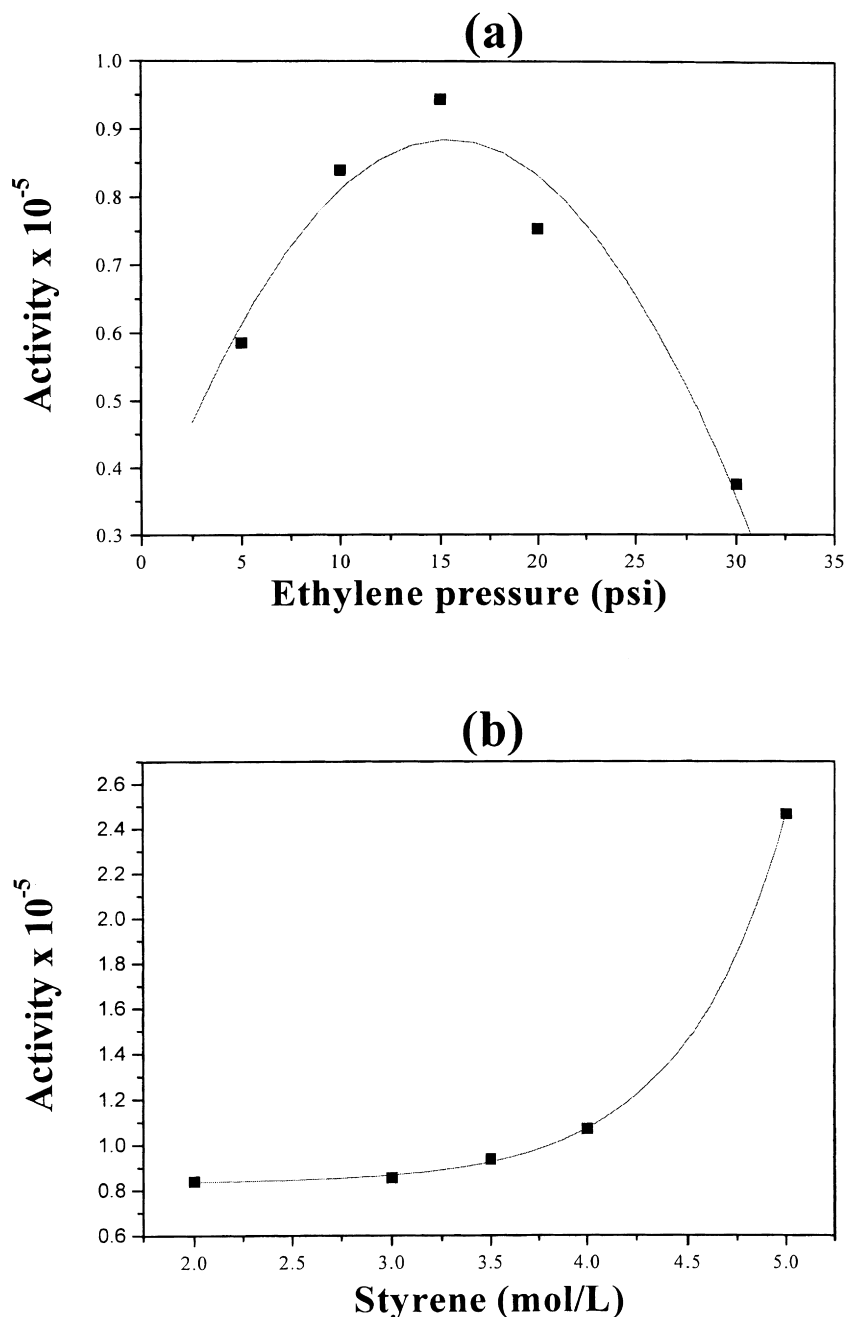Although the catalyst $C_5H_5TiCl_3$/MAO is not highly

(a)

(b)

Fig. 1. Activity as a function of: (a) PE pressure at constant temperature of 30°C; and (b) styrene concentration at a constant temperature and ethylene pressure at 10 psi.

catalytically active towards ethylene, copolymers are produced. Table 1 summarizes the productivity and the relevant run conditions. Run 1, s-PS homopolymer, serves as the reference. Runs 2–6 are performed under a constant styrene concentration (2 mol/L) and reaction temperature (30°C), but with increasing ethylene pressure. As shown in Fig. 1a, the activity varied from 3.75×10^4 (g/Ti mol h) to 9.44×10^4 (g/Ti mol h), which shows an initial increase followed by a subsequent decrease when ethylene pressure is higher than 15 psi. Runs 3,7,8,9 and 10 demonstrate the effects of styrene concentration at a constant ethylene

pressure (10 psi) and a constant reaction temperature (30°C). Contrasting with the ethylene pressure, the activity is found to increase continuously with increasing styrene concentration, as shown in Fig. 1b. Temperature effect on the activity is demonstrated in Runs 2 (30°C), 11 (15°C) and 12 (50°C) under a constant ethylene pressure (5 psi) and styrene concentration (2 mol/l). An increase of activity with increasing temperature is apparent.

The product is not homogeneous, rather it contains a mixture with substantial distribution of structure characteristics. To confirm the composition, the copolymers are first

Table 2
The fractionation by MEK and THF

Run no.	MEK-insoluble fraction (wt%)	THF-insoluble fraction (wt%)	THF-soluble fraction (wt%)
1	5.546	94.454	–
2	7.046	65.148	27.806
3	5.736	73.915	20.349
4	7.563	77.591	14.846
5	8.342	69.557	22.101
6	11.917	60.666	27.417
7	7.479	81.544	10.977
8	6.799	85.621	7.580
9	6.192	88.388	5.420
10	5.325	90.273	4.402
11	6.571	83.494	9.935
12	6.222	66.232	27.546

fractionated according to the solubility in MEK. Solution NMR shows that this fraction is mainly the atactic PS having a low molecular weight. The remaining portion (over 90 wt%) is subsequently fractionated by THF leading to the S- and I-fractions. The weight percentage of each fraction recovered are summarized in Table 2. In general, the MEK extracts are less than 8 wt% of the total production. The I-fraction contains from 65 to 94%, and the S-fraction contains from 4.4% to no more than 27% of the total copolymer product. It is also noted that both the PE homopolymer and the reference s-PS homopolymer are not soluble in THF. In addition, Run 2 (lowest ethylene pressure) and Run 12 (highest reaction temperature) contain as high as one quarter of the THF-soluble fraction.

3.2. Microstructure of the fractions

Molecular weight distribution for the four selected I-fractions is shown in Fig. 2. The approximate range of molecular weight M_w, however, lies between 2.8×10^4 (HI = 2.52) and 9.9×10^4 (HI = 2.25) Dalton using typical polystyrene standards. GPC for all the fractions show only a single molecular weight distribution with
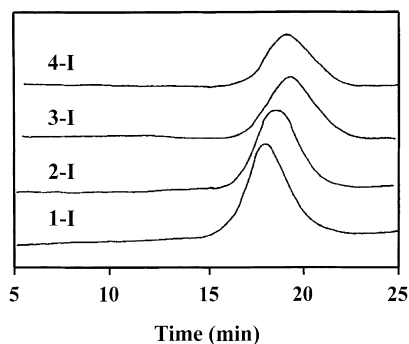

Fig. 2. GPC curves for four selected THF-insoluble fractions. The *x*-axis is presented in elution time due to the lack of GPC standards for the s-PS/PE copolymer. The rough range of molecular weight M_w lies from 9.9×10^4 (HI = 2.52) to 2.8×10^4 (HI = 2.25) Dalton.

a heterogeneity index less than 2.5. This result is in clear contrast with the THF-insoluble fraction reported by Xu et al. and by Oliva et al. [9,11] where bimodal molecular weight distribution (HI = 3.3) is attributed to the presence of both the s-PS and PE homopolymers. For the S-fraction, the GPC reveals that they are low molecular weight polymers.

^{13}C NMR characterized copolymer molecular characteristics include ethylene mole ratio ([E] mol%) and the tacticity for the copolymers in both fractions. Shown in Fig. 3 are the selected ^{13}C NMR solution spectra of the S-fraction. The region from 0 to 60 ppm shows mainly the methine CH (40.6–43.5 ppm) and methylene CH$_2$ (43.8–46.2 ppm) carbons from polystyrene and the backbone CH$_2$ (30.3 ppm) signals from polyethylene. The shift values differ slightly from those reported previously owing to slight difference in temperature for NMR measurements. The relative area of the methine and methylene resonances provides convenient means to quantify ethylene content [E] in each fraction. It is interesting to note that styrene tacticity [rr], in both I- or S-fractions, is all higher than 85%. In current polymerization conditions, ethylene does not deteriorate the styrene stereoregularity.

For the S-fraction, six minor peaks appearing at 34.3, 31.4, 29.4, 25.6, 21.2 and 14.1 ppm are detected. Their structural assignments are summarized in Table 3. These resonances are attributed to the triad units due to the frequent transitions between the styrene and ethylene units. The ethylene segment of the S-fraction contains short ethylene units with an average PE-block length calculated from the intensity of these "interfacial" resonances as follows:

$$N(\text{E-block}) \frac{2[\text{E}]}{[\text{ES}]} = 1 + 2 \frac{[\text{EE}]}{[\text{ES}]}.$$

This average E-block length is found to be less than 5 as summarized in Table 4. Interestingly, the resonances at 34.9 and 33.7 ppm, corresponding to the ethylene units bridged head-to-head with the styrene units,
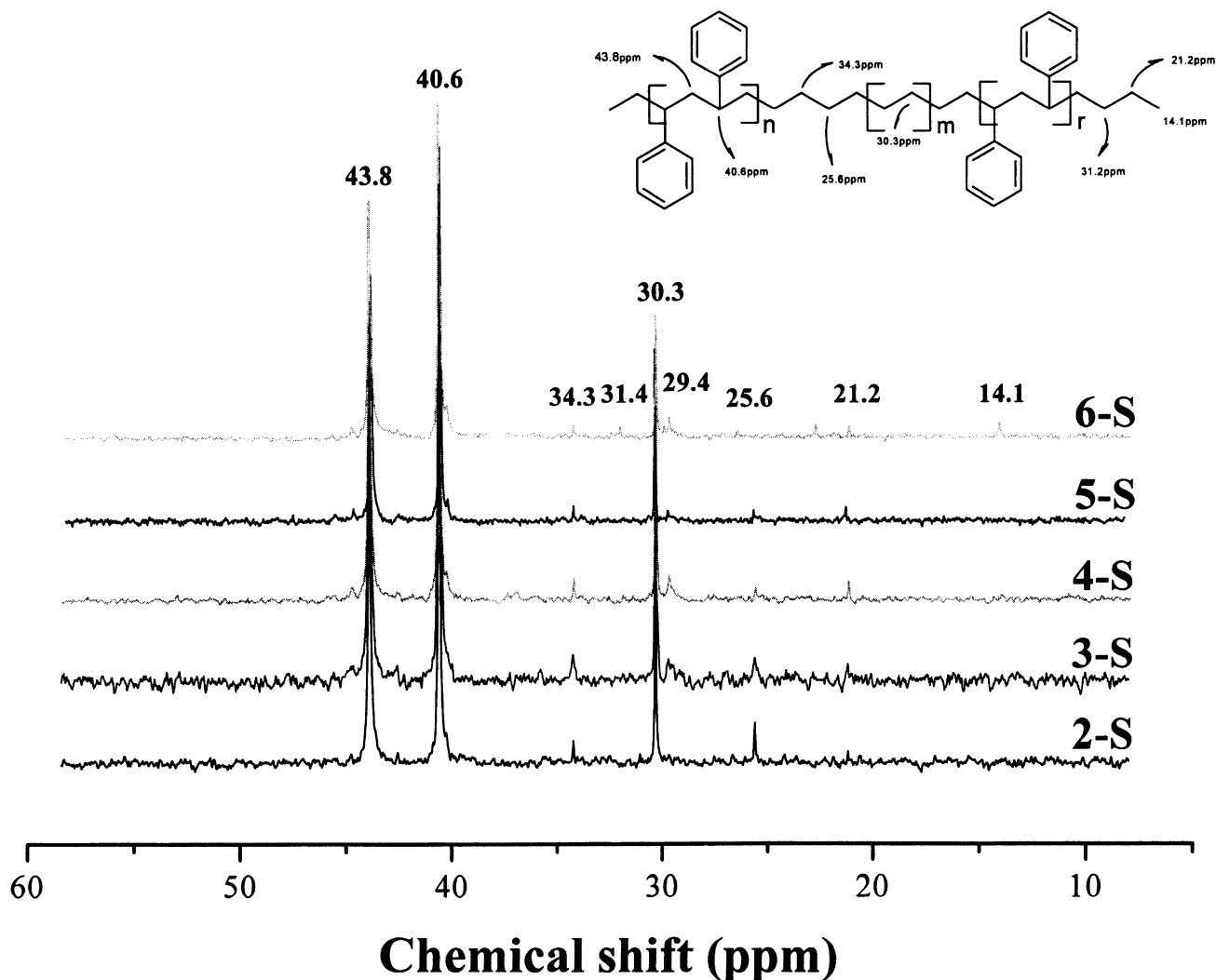
Fig. 3. The solution phase ^{13}C NMR spectrum recorded in chloroform at 300 K of the THF-soluble fraction for Runs 2–6 s-PS/PE copolymers.

Table 3
^{13}C Chemical shifts assignments

Carbon type[a]	Sequence[b]	S-fraction (300 K)	I-fraction (333 K)
$S_{\alpha\alpha}(CH_2)$	SSS	43.8	44.3
$S_{\alpha\alpha}(CH_2)$	ESS	–	–
$T_{\beta\beta}(CH)$	SSS	40.6	41.4
$T_{\beta\delta}(CH)$	ESS	–	–
$S_{\alpha\beta}$	SES*	34.3	–
$S_{\gamma\delta}$	EEE	30.3	30.3
$S_{\gamma\delta}$	SEE	29.4	–
$S_{\beta\beta}$	SES	25.6	–
$S_{\delta\delta}$	$CH_2(2s)^{*c}$	21.2	–
$P_{\delta\delta}$	$CH_3(1s)^{*c}$	14.1	–

[a] S: methene carbon; T: methine carbon; the Greek letter indicates the nearest methine carbon.

[b] E:ethylene unit; S: styrene unit.

[c] Chain end.

are completely absent. This precludes the regio-irregular SS configuration under current copolymerization. In a prior study using $C_5H_5Ti(Oh)_3$/MAO catalyst [9], the directionality is switched upon copolymerization with ethylene. We suspect the more violent reactivity with $C_5H_5Ti(Oh)_3$/MAO to be responsible for the irregular products (vide infra).

For the I-fraction, the NMR spectrum is simpler (Fig. 4). The signals from methine CH (41.4 ppm) and methylene CH_2 (44.3 ppm) carbons in polystyrene and the backbone CH_2 signals from polyethylene (~30 ppm) are all well resolved. However, the ^{13}C signals, corresponding to $S_{\alpha\delta}$, $S_{\beta\delta}$ "interfacial" carbon, would be much weaker as the s-PS and E-blocks are long. The solution ^{13}C NMR is fruitless in providing direct evidence for the long block structure, since binary mixture would yield essentially the identical spectra. Nevertheless, NMR fingerprints and GPC results for both fractions do not show appreciable inter-chain variations.

Table 4
Structural characteristics of the THF-soluble fraction

Run no.	[rr]	F = (PE mol%)	Average block (s-PS/PE)	T_g (°C)	T_m (°C)	ΔH (J/g)
2-S	87.2	8.10	11.35	94.30	263.27	25.53
3-S	89.9	9.30	9.750	97.68	260.53	26.50
4-S	87.7	12.3	7.130	95.81	263.74	24.71
5-S	88.5	16.9	4.920	92.99	262.66	20.67
6-S	88.9	18.8	4.320	92.39	259.73	27.86
7-S	–	–	–	97.69	261.49	27.62
8-S	–	–	–	97.45	259.45	25.37
9-S	–	–	–	86.82	257.46	14.56
10-S	–	–	–	88.17	249.88	15.01
11-S	–	–	–	93.33	263.36	14.75
12-S	–	–	–	96.46	261.27	24.5

NMR quantification shows that ethylene content is more than 8 mol% in the S-fraction but gives a wider variation of [E] value ranging from 1.3 to 21.2 mol% in the I-fraction (Table 5). Since shorter (thus non-crystallizable) ethylene units exhibit stronger salvation free energies with THF, the latter two fractions are resolved by their differences in THF solubility. The variation of styrene tacticity between I- and S-fractions is too small to account for the THF solubility difference.
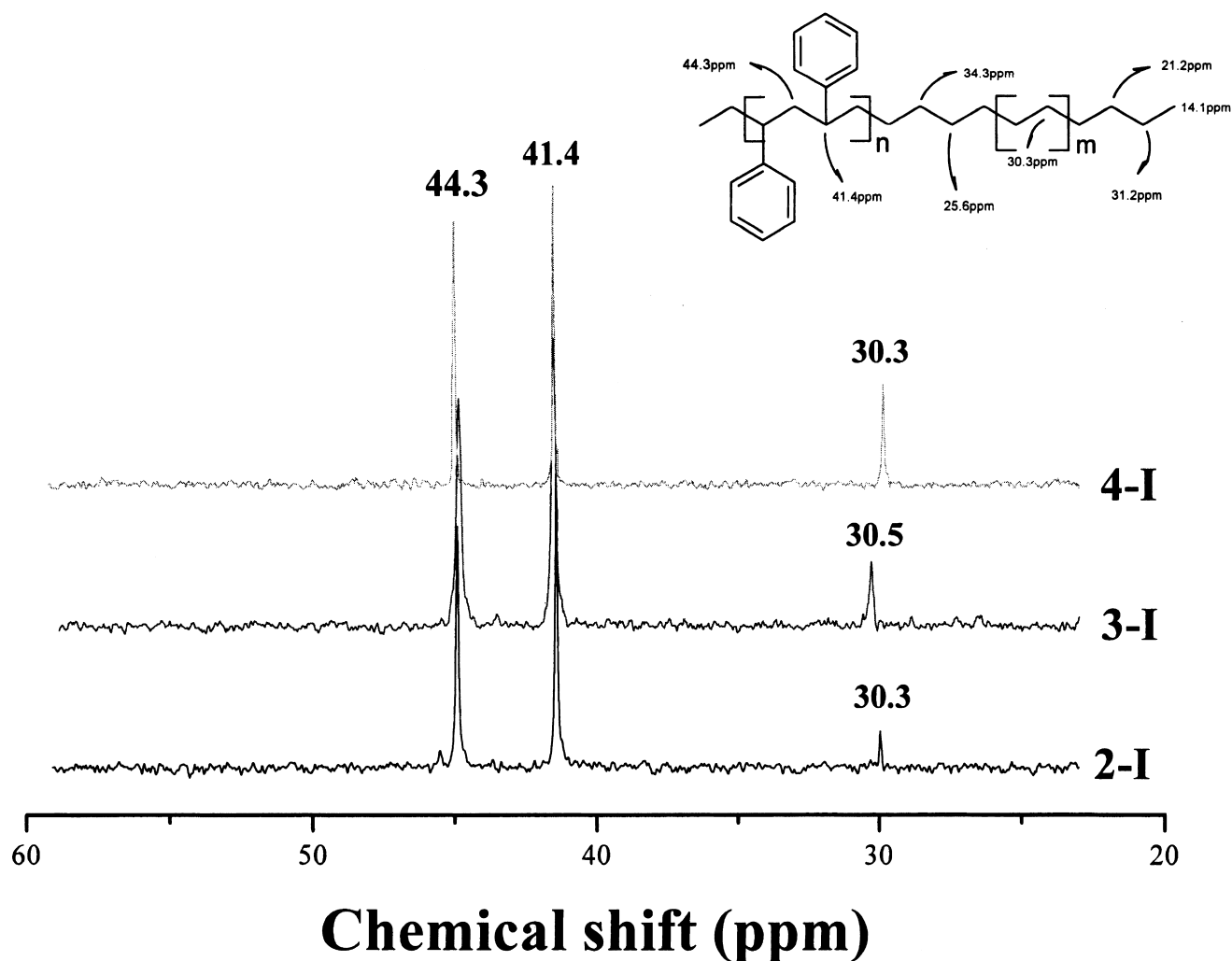

Fig. 4. The solution phase ^{13}C NMR spectrum recorded in trichlorobenzene at 333 K of the THF-insoluble fraction for Runs 2–4 s-PS/PE copolymers.

Table 5
Structural characteristics of the THF-insoluble fraction

Run no.	[rr]	F = (PE mol%)	T_g (°C)	T_m (°C)		ΔH (PE)	ΔH (s-PS)
1-I	98	0	102.21	–	261.3	–	11.55
2-I	98	1.30	100.03	–	263.2	–	23.16
3-I	98	4.10	99.85	126.3	261.8	0.16	23.63
4-I	98	7.80	104.33	123.8	262.5	2.02	24.48
5-I	98	11.9	101.77	123.9	261.5	3.21	24.96
6-I	98	21.2	102.57	124.6	262.9	5.81	22.03
7-I	–	–	102.43	125.0	262.3	0.21	27.03
8-I	–	–	102.16	–	263.0	–	27.79
9-I	–	–	100.61	122.6	260.9	–	26.39
10-I	–	–	102.46	–	260.7	–	26.59
11-I	–	–	102.87	–	263.0	–	24.61
12-I	–	–	102.97	–	261.5	–	23.05
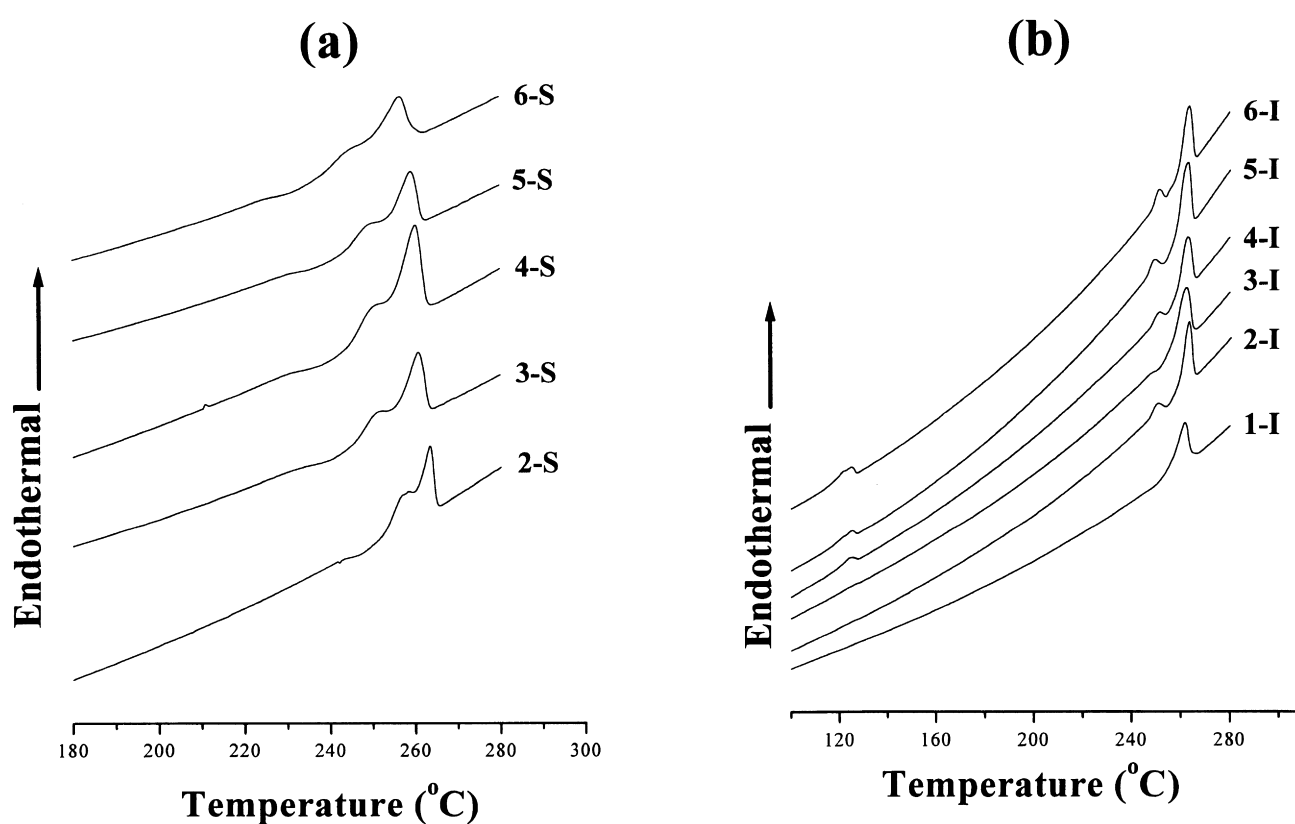
Fig. 5. Normalized DSC scans of: (a) THF-soluble fraction; and (b) THF-insoluble fraction of the s-PS/PE copolymer with different ethylene pressures.

3.3. Thermal analysis

DSC analysis of the copolymer gives a different thermodynamic behavior according to structural differences (ethylene length) in both I- and S-fractions with a high styrene content (>75 mol%). For the S-fractions, the melting trace shown in Fig. 5a for 2-S to 6-S exhibits two endothermic peaks around 240–260°C corresponding to the s-PS block structure. However, no trace of PE endotherm at temperatures below 130°C is observed, consistent with the structure characteristics that ethylene

block is too short (less than five ethylene units) to exhibit PE crystallinity.

In contrast, I-fractions show substantially different DSC traces from that of the S-fraction. Fig. 5b shows the normalized DSC traces for 1-I (pure s-PS) to 6-I, where two groups of melting endotherm occur in the neighborhood of ~261 and ~125°C. Here, the ethylene block is sufficiently long to exhibit the PE melting characteristics. The ethylene melting peak height increases with ethylene feed pressure indicating a higher [E] content in the copolymers. This is consistent with the results from NMR. Notice a lower temperature
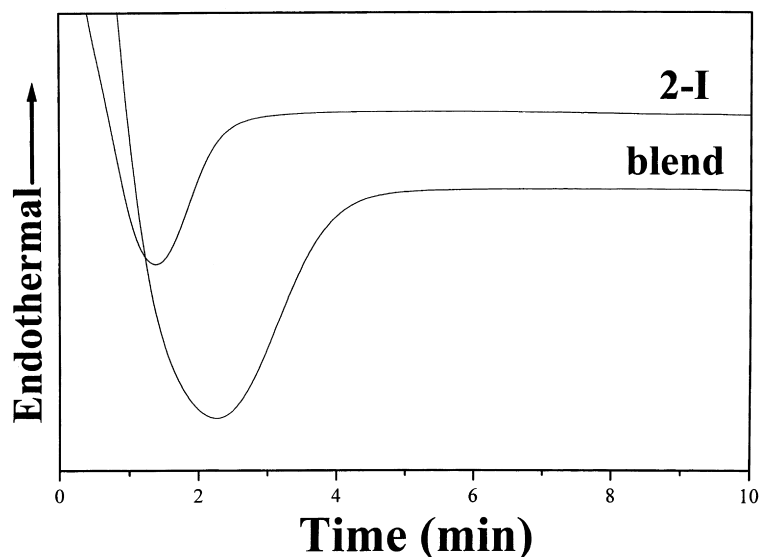
Fig. 6. Endotherm of isothermal crystallization for: (a) 2-I fraction; and (b) s-PS/PE mixture with [E] = 1.3 mol%.

shoulder peak at 248–250°C grows gradually with increasing ethylene content,[1] and hardly detectable for the pure s-PS under similar heat treatment [14,15]. Interestingly, the melt peak for the S-fraction (~250°C) also grows gradually with decreasing [E], but now with a much narrower peak width. This behavior is related to either (or both) a more rapid crystallization rate or structural homogeneity in the S-fraction. These distinctive differences in crystallization behaviors between I-, S-fraction and s-PS homopolymer cannot be accounted by molecular weight differences, but by fundamental structural uniqueness.

Shown in Fig. 6 are the variation of endotherm with time during isothermal crystallization at 135°C for sample 2-I ([E] = 1.2%) and the blend of 1-I and PE having the same composition as 2-I. The two samples have approximately identical s-PS stereoregularity and molecular weight. Interestingly, the crystallization half-time, where 50% of the full crystallinity is reached, differs sharply for the two samples at 0.76 min (2-I, $k =$ 1.21) and 1.27 min (blend, $k = 1.80$), respectively. The dramatic reduction of crystallization half-time of 2-I suggests that the copolymer bears a more rapid crystallization rate than that in the blend and provides direct evidence that it is not a binary blend of s-PS and PE. The results are sufficient to justify that I-fraction is not an s-PS and PE dual component mixture, but has a structure substantially different from a blend.

Difference in thermal degradation behavior also suggests that the I-fraction bears a structure uniquely different from the binary mixture of the s-PS and PE homopolymer. Fig. 7a shows the TGA traces for Runs 2-S ([E] = 8.1 mol%), 3-S ([E] = 9.3 mol%) and 6-S ([E] = 18.8 mol%). Fig. 7b

shows the corresponding traces for 1-I (s-PS homopolymer), 2-I ([E] = 1.3 mol%), 3-I ([E] = 4.1 mol%) and 6-I ([E] = 21.2 mol%). Regardless of the ethylene content, the S-fraction shows a rapid degradation within a narrow temperature around 340°C, while the I-fraction shows a gradual degradation beginning as early as ~200°C. In the S-fraction, the onset of degradation temperature increases with increasing styrene content implying that the ethylene segments may actually facilitate the thermal degradation, possibly through formation of a more amorphous regime. For the I-fraction samples, high percentages of un-degraded material (about 20%) are found even after heating to over 800°C. The remaining black powder is collected and subsequently identified to be graphite. This degradation behavior, never reported in all previous copolymers, is closely related to the block structure of the s-PS/PE copolymer.

Finer fractions can be obtained with more fractionation steps such as the use of dual solvents with varying compositions or by combining it with the temperature rise evolution fraction. Nevertheless, the present fraction study is sufficient to confirm that copolymerization produces a mixture of polymers that contain: (a) atactic or low molecular weight portion (minor); (b) random copolymer where the s-PS block is separated randomly by short ethylene block (S-fraction, smaller than 25 wt%); and (c) s-PS/PE block copolymer (I-fraction, greater than 65 wt%) where s-PS and PE are chemically bonded.

4. Discussion

The wide distribution of structures is apparent from the

---

[1] Combined with separate X-ray studies, these two peaks are found to be beta crystalline modifications.
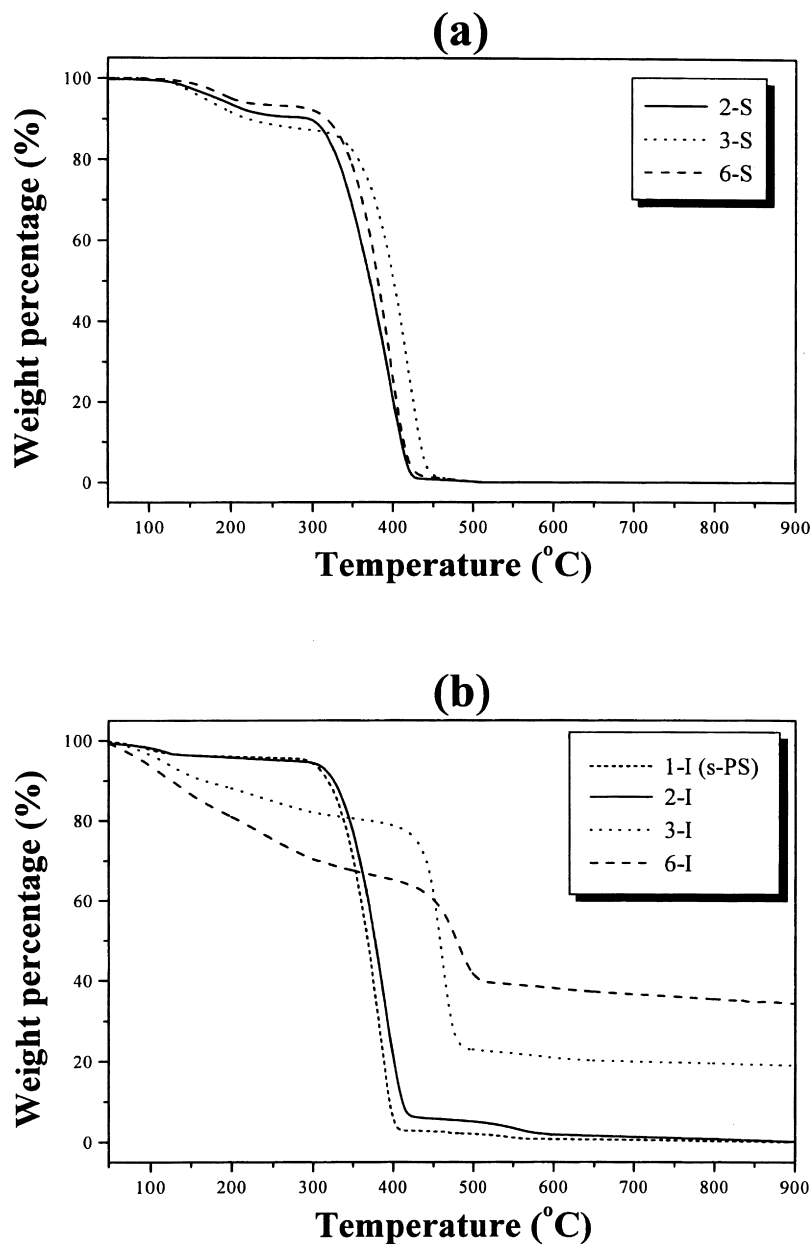
(a)

(b)

Fig. 7. TGA themalgram of: (a) 2-S, 3-S and 6-S; and (b) 1-I, 2-I,3-I and 6-I.

weight percentage in each fraction. As seen from Runs 2–6, increasing ethylene pressure gives more s-PS/PE block copolymers and less soluble fraction. Without ethylene, however, the S-fraction is completely absent. Apparently, ethylene is competing with styrene to yield a large quantity of the s-PS/PE copolymer with shorter PE segments separating the s-PS block. Fig. 8 shows the variations of the compositions in both I- and S-fractions with ethylene feed (mole ratio). In order to estimate the reactivity ratio, the ethylene feed pressure is converted to the ethylene feed concentration in the solution using a standard table for ethylene solubility in toluene solution at 30°C. For a homogenous product, reactivity ratios can be derived from the

Finnman–Ross relationship for chain growth.[2] It has been shown that the MAO-activated Titanocene is composed of multi-site characteristics with the presence of Ti(IV), Ti(III) and Ti(II) species.[3] Although the structures of the organometallic active center are under debate, several evidences show that $[C_5H_5Ti^{(IV)}R_2]^+$ is the catalyst for polyethylene, and $[C_5H_5Ti^{(III)}R]^+$ is the catalyst producing polystyrene

---

[2] The equation most generally used for copolymerization is $F_1 = (r_1 f_1^2 + f_1 f_2)/(r_1 f_1^2 + 2 f_1 f_2 + r_2 f_2^2)$.

[3] For comparison, Mulhaupt et al. [7] reported ethylene $r_E \sim 111$ and styrene $r_S \sim 0.055$, based on the results of titanium bis(phenolate) complexes.
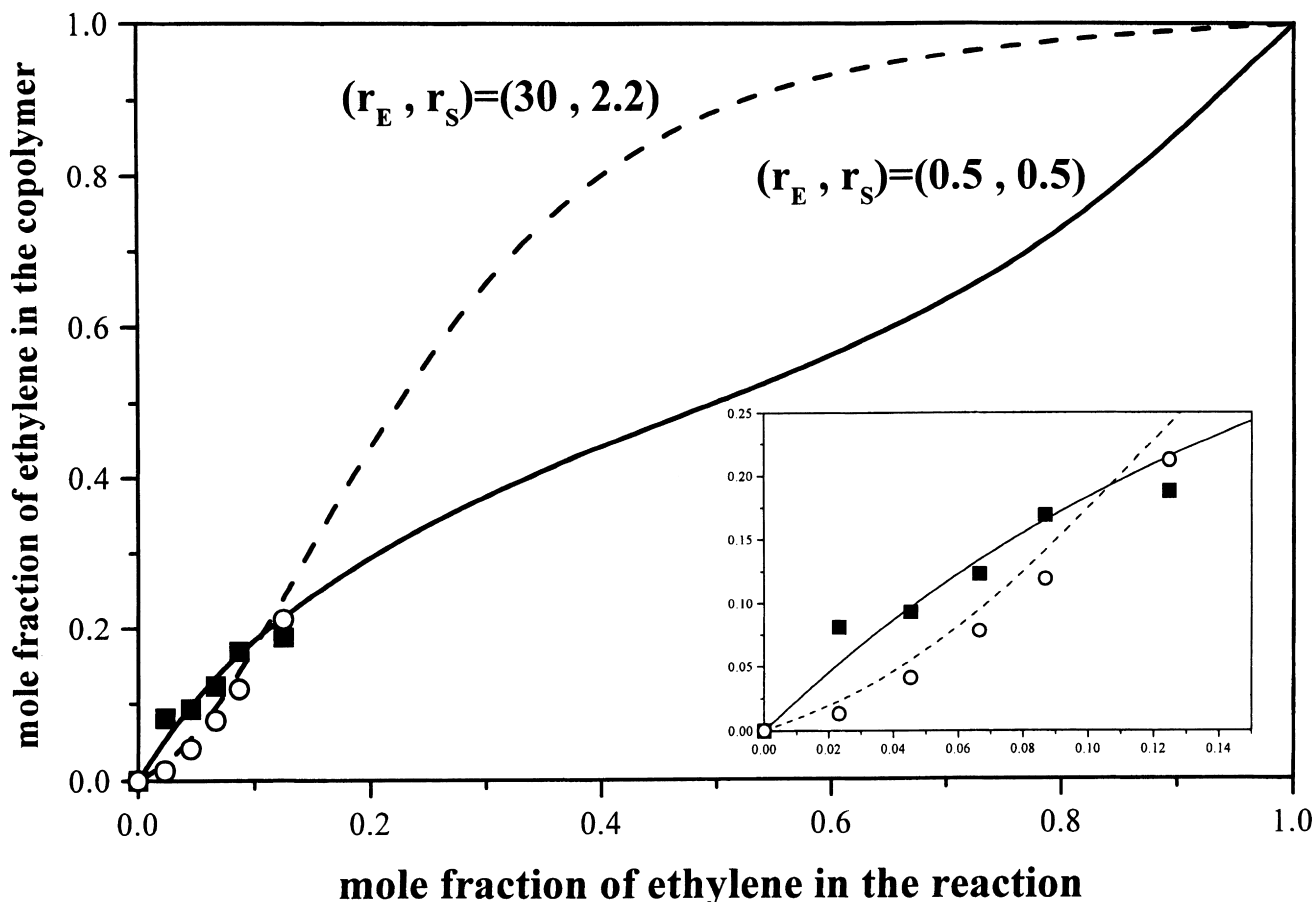
Fig. 8. Finnman–Ross plot of copolymer composition vs. ethylene feed pressure for the I- and S-fractions.

[16]. Along this line of derivation, there should exist a proper mechanism where switching between Ti(III) and Ti(IV) takes place during copolymerization. High concentration of MAO may provide the thermodynamic driving force in the presence of ethylene for such transitions, although direct evidence is not currently available.

With the possibility that multi-site characters occur in the MAO-activated catalyst system, we can treat the S- and I-fractions separately by assuming that they are produced according to two independent polymerization mechanisms. Using the adjusted ethylene feed ratio (f_1) and the ethylene content (F_1) in the products, we have derived the reactivity ratios for both fractions. For the I-fraction, $r_E = (30–20)$ and $r_S = (2.2–1.6)$, and for the S-fraction $r_E = (0.5–0.3)$ and $r_S = (0.5–0.2)$. In the S-fraction the product $r_E \times r_S$ is about 0.1, which is consistent with the random copolymer structure. For the I-fraction, the product $r_E \times r_S$ is much larger than 1 and consistent with a block copolymer structure [17]. As seen from Runs 3,7,8,9 and 10, increasing styrene concentration shows even more dramatic increase in weight fraction of the block type s-PS/PE. The copolymer composition vs. monomer feed composition gives a convex relationship and confirms that r_S should be much smaller than 3 as observed. Finally, it is observed that ethylene activity decreases more rapidly than that of the s-PS with

rising temperature, leading to an increase in the amount of the random type s-PS/PE. The concentration gradient between the gas and the liquid interface may be responsible for some degree of the heterogeneous structures, but not the major cause for the production of two types of copolymers shown in the present study.

Previous studies of the PS/PE copolymerization with high ethylene pressure with $C_5H_5Ti(OPh)_3$/MAO catalyst show that the THF-soluble fraction produces both random polystyrene/polyethylene copolymers with high stereoregularity in the styrene block, while the THF-insoluble fraction contains essentially a mixture made up of the s-PS and PE homopolymers [9,11]. In comparison, the present result gives rather different products with $C_5H_5TiCl_3$/MAO system where the THF-insoluble fraction is composed of the s-PS and PE block copolymers and the THF-soluble fraction is a copolymer with styrene block separated randomly with short PE segments. The present product also shows that a highly syndiotactic structure in SS chain segment is completely regio-regular. The results may imply that the $C_5H_5TiCl_3$ activated intermediates deliver better regio-specificity than with $C_5H_5Ti(OPh)_3$ or other bridged half-titanocene catalysts [18,19]. Additional copolymerization using $C_5H_5Ti(OPh)_3$ carried out under similar reaction conditions employed in this study shows that the block copolymer is

still produced, but the THF-insoluble weight fraction is reduced to below 30%. This difference is attributed to the fact that $C_5H_5TiCl_3$ has a lower ethylene activity ratio (r_E) than that for $C_5H_5Ti(OPh)_3$ and the possibility that switching between Ti(III) and Ti(IV) is easier to achieve with $C_5H_5TiCl_3$. Temperature and MAO content also influence the equilibrium of the active species, leading to variation in the population of the block and random type copolymer products. Although reducing the polymerization temperature ensures more blocked s-PS/PE copolymers, the productivity suffers and the molecular weight is lower than the homopolymer. In spite of the fact that the actual mechanism remains unclear, the sequential feed scheme coupled with the use of a lower reactivity metallocene catalyst with high MAO content leads to a higher percentage of copolymer product, which is block in nature.

5. Conclusion

The titanocene-based catalytic system of $C_5H_5TiCl_3$/MAO is capable of promoting the copolymerization of styrene and ethylene with a reasonable catalytic activity. THF fractionation resolved copolymer product into I- and S-fractions. Polystyrene segment remains highly stereoregulated and demonstrated crystallization behavior. A major fraction of the product existed as the block copolymer where the ethylene appears as the long block attached to s-PS. ^{13}C NMR characterization indicated that the styrene insertion is completely regio-regular with the $C_5H_5TiCl_3$/MAO catalyst system. Crystallization and thermal study confirm that the s-PS/PE block copolymers have morphology and structures substantially different from that of the s-PS/PE blend. The research clearly demonstrates that s-PS and PE-block copolymers with varying ethylene length are reachable with proper choice of catalyst, pretreatment conditions, temperature and controlled ethylene pressure.

References

[1] Koivumaki J, Fink G, Seppala JV. Macromolecules 1994;27:6254–8.
[2] Schneider MJ, Mulhaupt R. Macromol Chem Phys 1997;198:1121–9.
[3] Suhm J, Schneider MJ, Mulhaupt R. J Polym Sci, Polym Chem Ed 1997;35:735–40.
[4] Rossi A, Zhang J, Odian G. Macromolecules 1996;29:2331–8.
[5] Schneider MJ, Suhm J, Mulhaupt R, Prosenc M-H, Brintzinger H-H. Macromolecules 1997;30:3164–8.
[6] Leone O, Caporaso L, Pellecchia G, Zambelli A. Macromolecules 1995;28:4665–7.
[7] Sernetz FG, Mulhaupt R. Macromolecules 1997;30:1562–9.
[8] Ren J, Hatfield GR. Macromolecules 1995;28:2588–9.
[9] Xu G, Lin SL. Macromolecules 1997;30:685–93.
[10] Aaltonen P, Seppala J. Eur Polym J 1995;31:79–83.
[11] Oliva L, Mazza S, Longo P. Macromol Chem Phys 1996;197:3115.
[12] Spaleck W, Antberg M, Rohrmann J, Winter A, Bachmann B, Kioprof P, Behm J, Herrmann WA. Angew Chem 1992;104:1373.
[13] Bovey FA. Chain structure and conformation of macromolecules. Academic Press, 1982 (chap. 3).
[14] De Rosa C, Rapacciuolo M, Guerra G, Petraccone V. Polymer 1992;33:1423–8.
[15] Wang YK, Savage JD, Yang D, Hsu SL. Macromolecules 1992;25:3659–66.
[16] Chien JCW, Salajka Z, Dong S. Macromolecules 1992;25:3199.
[17] Grassi A, Saccheo S, Zambelli A, Laschi F. Macromolecules 1998;31:5588.
[18] Chien JCW, Hu Y. J Polym Sci Polym Chem Ed 1989;27:1989.
[19] Oliva L, Caporaso L, Pellecchia C, Zambelli A. Macromolecules 1995;28:4665–7.